Colorimetric and Photometric Modeling of Liquid Crystal Displays

Louis D. Silverstein
VCD Sciences, Inc., Scottsdale, Arizona

Thomas G. Fiske
Xerox Palo Alto Research Center, Palo Alto, California

Introduction

Liquid crystal displays (LCDs) are currently the leading candidate technology for the next generation of high-performance color workstations. Color LCD technology has been maturing at a rapid pace along with major improvements in display performance. This is at least in part due to large research and development expenditures focused on bringing color LCD technology to market. LCDs offer the extraordinary design flexibility of a light valve based device, while exhibiting the desirable characteristics of relatively low volume, weight, and power consumption. Moreover, with proper optimization of optical and electronic components, color LCDs are capable of color per-formance equal to or exceeding that of the venerable shadow-mask color CRT.

For a color CRT, the spectral composition and intensity of emitted light is a function of the excitation of phosphors by a stream of electrons emitted by a cathode. Since the intensity of emissions from each of the three primary color phosphors (R, G, and B) is directly proportional to the beam current while the spectral composition of the emission from each phosphor is invariant across beam current, the color and luminance of the color CRT are simply related to the luminous proportions of emitted light from each of the three primary color phosphors. There are generally no active optical elements involved, and the spectral composition of the output of the color CRT can be considered to be isotropic as well as homogenous across space and time. Thus, assuming that the spectral power distribution of the emissions from the R, G and B phosphors are known and suitably converted to tristimulus values (e.g. via the CIE 2º color matching functions), the colorimetric and photometric performance of the CRT may be readily characterized andoptimized in tristimulus space.

Unlike the color CRT, which is optically simple and thus relatively easy to model and optimize in terms of colorimetric/photometric performance, the color LCD is optically complex. A transmissive color LCD is composed of a source of illumination and a multitude of layer- ed optical elements which each modify the spectral composition of light originating from the source. Moreover, some of these elements, such as polarizers, retardation films and the liquid crystal (LC) layer itself, are optically anisotropic and birefringent layers which produce complex spectral modifications that vary as a function of the material parameters and construction of the LC cell, display voltage (i.e., luminance or gray level), and the direction of light propagation.

It should be apparent that the colorimetric modeling and optimization of an LCD is a much more complex task than comparable analyses for a color CRT. In this paper we describe the foundations of LCD operation, including some basics of LCD optical models and the effects of various LCD design parameters on the spectral, intensive, and angular propagation of light through an LCD. Further, we present a method for estimating the colorimetric and photometric characteristics of color LCDs which enables the investigation of the effects of variations in a number of critical color LCD components (e.g., spectral power distribution of the source of illumination, color filter dye concentration and thickness, LC birefringence, and LCD cell construction geometry) on the ultimate chromaticity and luminance rendering capabilities of the display. Finally, we present both modeled and empirical data on the color performance of today's state-of-the-art color LCDs, compare this performance with that of existing color CRTs, and discuss the promises and problems of this new generation of high-performance color imaging devices.

Fundamentals of Color LCD Operation

Some Basic Concepts of Liquid Crystals

Liquid crystals are complex, anisomeric organic molecules which, under certain temperature conditions, exhibit the fluid characteristics of a liquid and the molecular orientational order characteristics of a solid.[1] A consequence of the ordering of anisomeric molecules is that LCs exhibit mechanical, electric, magnetic and optical anisotropy.[2,3] There are many different types of LCs and display optical configurations to take advantage of their unique optical characteristics. It is important to recognize that most LC materials are uniaxial and birefringent. Uniaxial materials possess one unique axis, the optic axis, which is parallel to the liquid crystal director (i.e., the long axis of the molecules). The anisotropic nature of LC materials gives them the optical property of birefringence, which refers to the phenomenon of light traveling with different velocities in crystalline materials depending on the propagation direction and the orientation of the light polarization relative to the crystalline axes.2 For a uniaxial LC, this implies different dielectric constants and refractive indices for the unique or "extraordinary "direction and for other "ordinary" direc-

tions in the LC material. The most widely used LC phase is the nematic type, which is shown Figure 1 along with its principle axes and associated dielectric and optical parameters.[4]

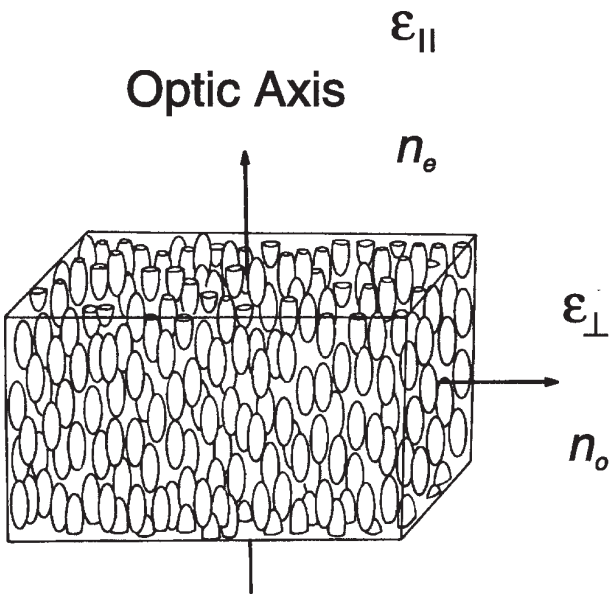

Figure 1. Nematic LC with principal axes and associated dielectric and optical parameters

Definitions of the basic parameters which determine the electrical and optical performance of the LC are provided in Equation (1), which also describes the phase difference between polarization components produced by the birefringence and path length through the LC layer.[3,4]

For a positive uniaxial material

$$\Delta\varepsilon = \varepsilon_{||} - \varepsilon_{\perp}$$

$$\Delta n = n_e - n_o$$

$$P_d = \frac{2\pi\Delta n d}{\lambda}$$

Where:

$\varepsilon_{||}$ = dielectric constant || to the LC director

$\varepsilon_{\perp}$ = dielectric constant ⊥ to the LC director

n_e = refractive index || to the LC director

n_o = refractive index ⊥ to the LC director

$\Delta\varepsilon$ = dielectric anistropy

Δn = birefrengence

λ = wavelength

d = LC layer thickness

P_d = phase difference of polarization components

The predominant LC cell configuration for high-performance color LCDs is the twisted-nematic cell. In the TN cell, incoming light is initially linearly polarized by an entrance polarizer and then the axis of polarization is optically rotated by the LC layer. The typical twist or rotation angle used for most TN LCDs is 90°, although other twist angles may be used to achieve certain desired optical characteristics.[3] After optical rotation by the LC layer, the polarization state of light exiting the LC layer is analyzed by the exit polarizer or "analyzer." Two principle configurations of TN cell entrance and exit polarizers are used, LCDs that utilize crossed polarizers are often called normally-white (NW) mode LCDs while those consisting of parallel polarizers are typically called normally-black (NB) mode LCDs. Figure 2 illustrates the basic principles of operation of a TN cell operated in the NW mode.

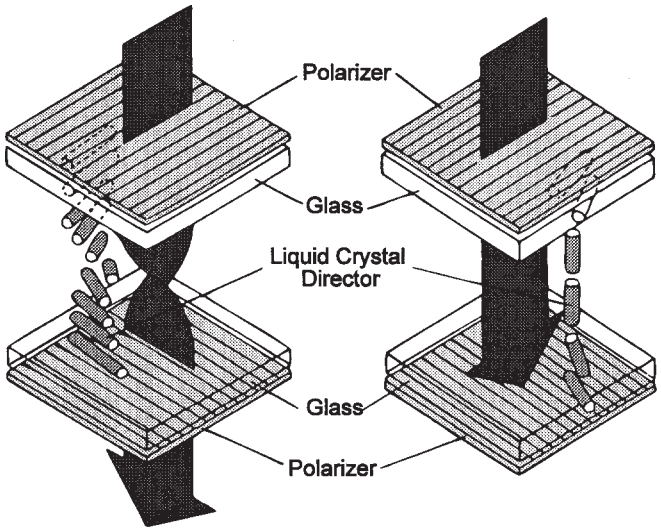

Figure 2. Basic principles of operation of a TN LC cell operated in the NW mode

It is important to recognize two fundamental concepts of TN cell operation. First, is the fact that the transmis- sion of the TN cell is a function of the efficiency of the initial polarization of light, transformation of the polarization state via optical rotation by the LC layer, and analysis of the final state by the TN cell analyzer. Light polarization relates to the electric field vibation transverse to the direction of light propagation and can always be described as the vector sum of two orthogonal polarization vectors.[5] As such, the polarization state of light exiting the LC cell will be a function of those parameters which alter the phase relations between the polarization components, i.e., the LC birefringence, LC layer thickness, twist angle and wavelength. Elliptical polarization is the general case, while linear and circular polarization are special forms occurring at relative phase differences of 0 and $\pi/2$ between the two polarization components, respectively.[5] Second, as de-

fined in Equation (1), the relative phase differences between polarization components vary as a function of wavelength. This implies that for a TN cell with a given LC birefringence and layer thickness, linear polarization after optical rotation can only be achieved at a discrete series of wavelengths with the polarization state at other wavelengths exhibiting some degree of ellipticity. Thus, minima and maxima of cell transmission can only be achieved at a discrete series of wavelengths and some degree of spectral "leakage" occurs at other wavelengths.[6]

Spectral Tuning of LCDs

Figure 3 shows the major optical components of a color LCD and their spectral tuning characteristics. It can be seen that the color LCD is composed of a backlight illumination source with a specific spectral power distribution, linear polarizers, glass sheets, thin-film indium-tin-oxide (ITO) electrodes, absorbing thin-film color selection filters, and an optically active layer of birefringent LC material. Incoming light from the illumination source is initially plane polarized by the rear or entrance polarizer and then passes sequentially through the series of optical elements. Each optical element modifies the spectral composition of light passing through it.

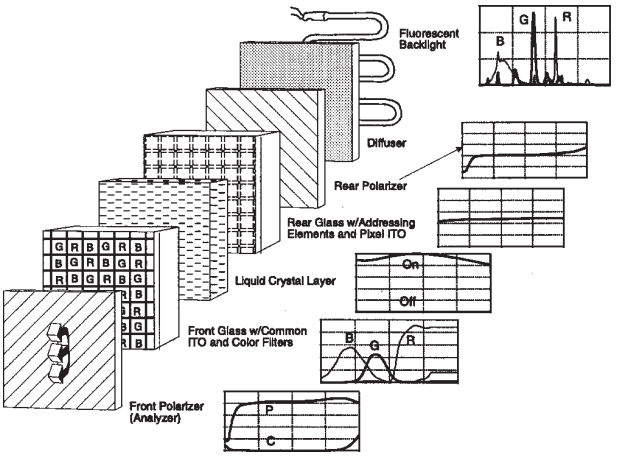

Figure 3. Major optical components of a color LCD and their spectral tuning characteristics

At this stage in the colorimetric/photometric modeling and optimization of a color LCD, each LCD component must be characterized by its full emission or transmission spectrum. While the isotropic elements are subject to typical path length effects and wavelength-dependent interference effects occur in the thin-film layers (e.g., ITO electrodes), complex spectral modifications occur as light propagates through the anisotropic, birefringent polarizer and liquid crystal layers. These modifications are critical-ly dependent on the material parameters and construc- tion of the liquid crystal cell, display voltage (i.e. luminance or gray level), and the direction of light propagation.

Properties for three of the optical components of the color LCD will have the principle effects on the ultimate colorimetric and photometric characteristics of the display: the spectral power distribution (SPD) of the illumination source; the spectral transmission of the thin-film color selection filters; and the selection of the LC material and tuning of the LC cell gap.[7] Here we consider aspects the spectral tuning of each of these elements.

Most direct-view color LCDs utilize either hot-cathode (HCF) or cold-cathode (CCF) fluorescent lamps for backlight illumination. Tri-band phosphor mixtures are typically employed to improve color performance for these lamps. For a tri-band HCF or CCF source, a variety of color phosphors can be utilized and then the SPD of the lamp can be tuned approximately by the following simple relations:[7]

$$S_{src}(\lambda) = P_r S_r(\lambda) + P_g S_g(\lambda) + P_b S_b(\lambda) + S_{ml}(\lambda)$$

Where:

S_{src} = SPD of the source

$S_r(\lambda)$= SPD of the R component

$S_g(\lambda)$= SPD of the G component

$S_b(\lambda)$= SPD of the B component

$S_{ml}(\lambda)$= SPD of the visible mercury lines

P_x= Proportion of the R, G, or B component

Direct-view color LCDs typically utilize thin-film color absorption filters to accomplish primary color selection. The variety of dyes and pigments which are compatible with LC materials and the LCD manufacturing pro-cess are limited. Thus, there are limited degrees of freedom for tailoring the spectral transmission of thin-film color filters. Once the particular filter materials are selected, filter thickness and dye concentration can be adjusted within a range compatible with thin-film deposition processes. If the spectral transmission of a set of reference filter materials is known, and the dye or pigment in concentration is known to follow Beer's Law within the range of concentrations used, then the spectral transmission of the filter material at other dye concentrations and film thicknesses may be estimated via the use of the Beer-Lambert Law as follows:[7,8]

$$T_r(\lambda) = T_{r\text{-}ref}(\lambda)^{\gamma}$$
$$T_g(\lambda) = T_{g\text{-}ref}(\lambda)^{\gamma}$$
$$T_b(\lambda) = T_{b\text{-}ref}(\lambda)^{\gamma}$$

Where:

$T_{x\text{-}ref}(\lambda)$ = trans. of reference R, G, or B filter[3]

$d_{x\text{-}ref}$= dye conc. of ref. R, G, or blue filter

$t_{x\text{-}ref}$ = thickness of ref. R, G, or B filter

d_x = desired dye conc. of R, G, or B filter

t_x = desired thickness of R, G, or B filter

γ = $(d_x/d_{x\text{-}ref})\ (t_x/t_{xref})$

The design trade-offs for adjusting color filter thickness and/or dye concentration will, of course, be a change in the light throughput efficiency of the LCD.

The LC cell gap is a critical parameter for tuning the color performance, luminance and contrast ratio of a color LCD.[6,7] As mentioned in the previous section, for any given LC birefringence and LC cell gap, maxima and minima of cell transmission can only be achieved at a specific series of discrete wavelengths. The cell gap may be selected such that LCD contrast ratio, color gamut or color saturation are maximized or according to some weighted combination of display metrics. Figure 4 illustrates the effects of varying the cell gap on the transmission of the on- and off-states of a binary LCD. We have assumed ideal polarization to emphasize transmission variation with wavelength, and only the optically active state for each mode is shown.

Figure 4. LC cell transmission as a function of wavelength and cell gap

The following set of equations may be used to determine the spectral tuning characteristics of the LC layer for a binary color LCD viewed on-axis:[6,7]

For the NB mode:

$$T_{lc-off}(\lambda) = \frac{\sin^2[\theta(1+u^2)^{1/2}]}{(1+u^2)} + T_{xp}(\lambda)$$

$$T_{lc-on}(\lambda) = \sin^2\theta$$

For the NW Mode:

$$T_{lc-off}(\lambda) = 1 - (\sin^2\theta) + T_{xp}(\lambda)$$

$$T_{lc-on}(\lambda) = 1 - \frac{\sin^2[\theta(1+u^2)^{1/2}]}{(1+u^2)} \qquad (4)$$

Where:

$$u = \frac{\pi d_{lc}\Delta n(\lambda)}{\theta\lambda}$$

θ = twist angle in radians

d_{lc} = cell gap

$\Delta n(\lambda) = n_e(\lambda) - n_o(\lambda)$

$n_e(\lambda)$ = extra-ordinary refractive index of LC

$n_o(\lambda)$ = ordinary refractive index of LC

$T_{xp}(\lambda)$ = transmission of crossed polarizers

A Simplified Colorimetric Model for Binary Color LCDs Viewed On-Axis

A great deal of colorimetric/photometric analysis and optimization for LCDs can be accomplished with a reduc-ed optical model for binary or bi-level displays viewed normal to the display surface. We have recently developed a simplified colorimetric model for binary LCDs and have applied the model successfully to the development of several prototype color LCDs.[7] While this reduced model does not allow for intermediate LC cell voltage states or estimates for off-axis directions of light propagation, it does enable efficient spectral tuning of the illumination source, LC parameters and principle LCD material layers. The basic equations for the SPDs of red LCD pixel elements in both the on- and off-states are given in Equation (5). Similar equations are required for the pixel elements of the other primary colors.

$$R_{on}(\lambda) = S(\lambda)\, T_{p\text{-}ent}(\lambda)\, T_{g\text{-}ent}(\lambda)\, T_{lc\text{-}on}(\lambda) \times T_{red\text{-}f}(\lambda)\, T_{g\text{-}exit}(\lambda)\, T_{p\text{-}exit}(\lambda)\, T_{oe}(\lambda)$$

$$R_{off}(\lambda) = S(\lambda)\, T_{p\text{-}ent}(\lambda)\, T_{g\text{-}ent}(\lambda)\, Y_{lc\text{-}off}(\lambda) \times T_{red\text{-}f}(\lambda)\, T_{g\text{-}exit}(\lambda)\, T_{p\text{-}exit}(\lambda)\, T_{oe}(\lambda)$$

Where:

$S(\lambda)$ = SPD of illumination source

$T_{g\text{-}ent}(\lambda)$ = transmission of entrance glass (w/ITO and alignment layer) (5)

$T_{p\text{-}ent}(\lambda)$ = transmission of entrance polarizer

$T_{lc\text{-}on}(\lambda)$ = as defined in Equation (4)

$T_{lc\text{-}off}(\lambda)$ = as defined in Equation (4)

$T_{x\text{-}f}(\lambda)$ = transmission of color filter

$T_{g\text{-}exit}(\lambda)$ = transmission of exit glass

$T_{p\text{-}exit}(\lambda)$ = transmission of exit polarizer

$T_{oe}(\lambda)$ = transmission of other optical elements

Having calculated the SPDs of the LCD primary color pixels, we can now transform these quantities into CIE tristimulus values[8] and calculate the luminance of the primary color pixels. Again, here we

$$X_{r-on} = \int_{380}^{780} R_{on}(\lambda)\bar{x}(\lambda)d(\lambda), X_{r-off} = \int_{380}^{780} R_{off}(\lambda)\bar{x}(\lambda)d(\lambda)$$

$$Y_{r-on} = \int_{380}^{780} R_{on}(\lambda)\bar{y}(\lambda)d(\lambda), Y_{r-off} = \int_{380}^{780} R_{off}(\lambda)\bar{y}(\lambda)d(\lambda)$$

$$Z_{r-on} = \int_{380}^{780} R_{on}(\lambda)\bar{z}(\lambda)d(\lambda), Z_{r-off} = \int_{380}^{780} R_{off}(\lambda)\bar{z}(\lambda)d(\lambda)$$

$L_{r\text{-}on} = 683\ Y_{r\text{-}on}$ $\qquad$ $L_{r\text{-}off} = 683\ Y_{r\text{-}off}$

Where:

$\bar{x}, \bar{y}, \bar{z}$ = CIE 1931 color matching functions
$L_{x\text{-}xx}$ = luminance in cd/m^2

calculate the tristimulus values of the red pixel elements only. Similar calculations are required for the other primary color pixel elements. Finally, we must calculate a weighted combination of the pixel element tristimulus values to convert these quantities to space-average tristimulus values. The space-average values enable us to account for the aperture ratio of the display, the color pixel mosaic and the non-zero luminance or "leakage" for off-state pixels.

$$X_{r\text{-}sa} = A_r[(R_aX_{r\text{-}on}) + G_aX_{g\text{-}off}) + (B_aX_{b\text{-}off})]$$

$$Y_{r\text{-}sa} = A_r[(R_aY_{r\text{-}on}) + G_aY_{g\text{-}off}) + (B_aY_{b\text{-}off})]$$

$$Z_{r\text{-}sa} = A_r[(R_aZ_{r\text{-}on}) + G_aY_{g\text{-}off}) + (B_aZ_{b\text{-}off})]$$

$$L_{r\text{-}on\text{-}sa} = 683\ Y_{r\text{-}sa}$$

$$X_{g\text{-}sa} = A_r[(R_aX_{r\text{-}off}) + G_aX_{g\text{-}on}) + (B_aX_{b\text{-}off})]$$

$$Y_{g\text{-}sa} = A_r[(R_aY_{r\text{-}off}) + G_aY_{g\text{-}on}) + (B_aY_{b\text{-}off})]$$

$$Z_{g\text{-}sa} = A_r[(R_aZ_{r\text{-}off}) + G_aY_{g\text{-}on}) + (B_aZ_{b\text{-}off})]$$

$$L_{g\text{-}on\text{-}sa} = 683\ Y_{g\text{-}sa} \qquad (7)$$

$$X_{b\text{-}sa} = A_r[(R_aX_{r\text{-}off}) + G_aX_{g\text{-}off}) + (B_aX_{b\text{-}on})]$$

$$Y_{b\text{-}sa} = A_r[(R_aY_{r\text{-}off}) + G_aY_{g\text{-}off}) + (B_aY_{b\text{-}on})]$$

$$Z_{b\text{-}sa} = A_r[(R_aZ_{r\text{-}off}) + G_aY_{g\text{-}off}) + (B_aZ_{b\text{-}on})]$$

$$L_{b\text{-}on\text{-}sa} = 683\ Y_{b\text{-}sa}$$

Where:

A_r = display aperture ratio

R_a, G_a, B_a = active area for R, G, and B pixels

$X_{*\text{-}sa}, Y_{*\text{-}sa}, Z_{*\text{-}sa}$ = space-average tristimulus values

To evaluate the accuracy of our reduced LCD colorimetric model, we compared the modeled space-average chromaticity coordinates of the display primaries and white point for an early color LCD prototype with spectroradiometric measurements of the assembled display. The disp-lay was an active-matrix color LCD operated in the NW mode. The approximate display active area was 8.64 cm × 7.37 cm and a RGB delta-triad mosaic of color filters was used. For this early prototype, a standard HCF lamp was used as an illumination source and thus did not contain a tri-phosphor blend which was optimized for the thin-film color filters or LC parameters. A comparison of the modeled and measured chromaticity coordinates for this color LCD, shown in Figure 5, reveals a close correspondence between predicted and measured colors. A small discrepancy is evident for the G primary, which also results in a small error for the white point. In general, small errors of this nature can often be attributed to slight changes in material characteristics and/or geometry occurring during fabrication and assembly of the completed display. The color gamut of a typical CRT monitor with P-22 phosphors is shown in Figure 5 to provide a color performance reference.

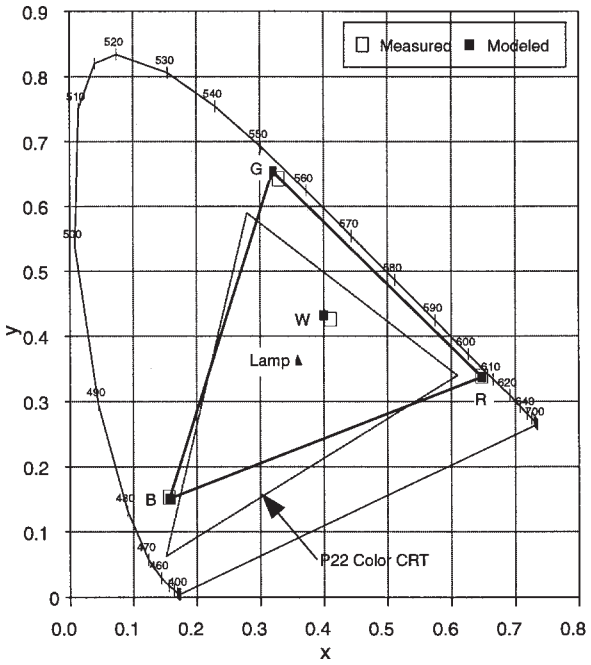

Figure 5. A comparison of modeled and measured chromaticity coordinates for an early prototype color LCD

Voltage-Controlled Gray Scale and Off-Axis Viewing in LCDs

For both voltage-controlled gray scale and off-axis viewing, the light path through the LC layer "sees" a different birefringence than in the fully voltage-saturated, on-axis situation.[4,9] This is due to the fact that the angles at which the light path intercepts the anisotropic LC molecules vary as a function of LC cell voltage and viewing angle. This in turn results in different degrees of stimulation of the ordinary and extraordinary modes of the LC causing varying degrees of phase difference between the two polarization components, different polarization states at exit from the LC cell, and resulting variations in light transmission through the exit polarizer. As described

earlier, phase differences between polarization components are wavelength dependent, thereby resulting in chromaticity differences as well intensity or luminance differences. Off-axis viewing adds additional complications due to path length differences through all of the material layers comprising the LCD as well as angle-related reflection and polarization effects at all of the different optical boundaries.

Modeling LCD optical transmission as a function of LC cell voltage and/or viewing angle requires much more complex material optics calculations for layered media. The spectral transmission, reflection and polarization state through each layer and across each optical boundary must be computed. The two principle approaches applied to the optical modeling of generalized LC structures are the 2×2 Jones matrix approach[10,11,12] and the more complex 4×4 propagation matrix approach.[13,14,15] The Jones matrix is a common tool for the analysis of birefringent optical systems. It is fast and efficient, but does not inherently account for Fresnel reflections at optical boundaries or Fabry-Perot interference effects in thin optical layers. The 4×4 propagation matrix approach, on the other hand, is much more computationally intensive but provides an exact solution which accounts for all reflections and interference effects.

Regardless of which approach to the layered optical calculations is used, the LC layer can no longer be treated as a single birefringent optical element but must be subdivided into a number of "homogenous" sub-layers and the orientation of the LC molecules (and thus the birefringence) estimated within each sub-layer as a function of applied LC cell voltage. Calculation of the local LC director orientation within each sub-layer requires complex numerical methods for fluid dynamics.[3,16] The input parameters include the dielectric, elastic and viscosity constants of the LC material, layer thickness, helical pitch of the LC material, and the applied voltage. The result is a set of electro-distortion curves which describe the local tilt (θ) and twist (Φ) angles of the LC director as a function of distance through the LC layer and voltage [usually specified as a reduced voltage denoting applied voltage (V) divided by the threshold or critical voltage (V_c)) of the LC material]. Figure 6 shows a set of electro-distortion curves for a specific LC material at a layer thickness of 5.3 microns and a range of V/V_c from 1 to 3 reduced volts.

For the remainder of this paper, we will concentrate our discussion on modeled on-axis performance for an optimized, gray-scale color LCD. We adopt this focus for two reasons. First, we have previously addressed key issues in off-axis color and contrast performance for LCDs.[17] Second, we seek to explore the limits of the color gamut, stability of pixel chromaticity, and color tracking performance across gray levels for today's state-of-the-art in color LCD technology and materials. We believe that such an analysis is critical for determining the suitability of color LCD technology for high-performance color imaging applications and to assess its potential compared to high-end color CRT monitors.

To achieve these objectives, we have used a 4×4 propagation matrix approach[13] to model the colorimetric and photometric performance of an active-matrix LCD with 8 linear voltage-controlled gray levels operated in the NW mode. The optical components of the model LCD are all available materials, and we have optimized the HCF illumination source, thin-film color filters, and LC cell parameters as discussed previously. The model display utilizes a RGBG quad mosaic of color filters in part to reduce the impact of spectral contamination caused by the sidebands of the G phosphor emissions spreading into the spectral passbands of the R and B color filters.

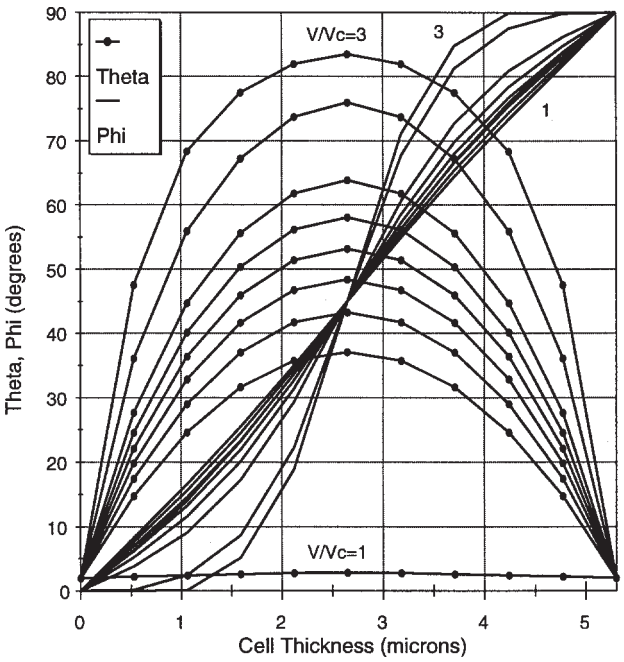

Figure 6. Calculated electro-distortion curves for a specific LC material and a cell thickness of 5.3 microns.

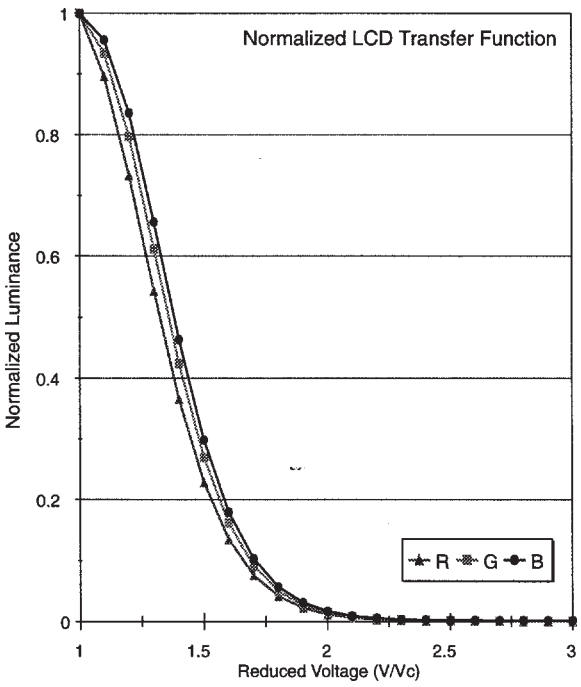

Figure 7. Normalized voltage-to-luminance transfer functions for the modeled NW-mode color LCD

To develop the 8 linear gray levels for the model display, we first determined V_c for the display by application of numerical methods for LC fluid dynamics.[16] Having obtained an estimate of V_c, we then calculated the electro-distortion functions for V/V_c in the range of 1 to 3 reduced volts at a sampling interval of .1 reduced volts. These electro-distortion functions were then used with the 4 × 4 layered optics calculations for the complete model LCD to generate normalized voltage-to-luminance trans-fer functions for the R, G, and B LCD pixel elements, which are shown in Figure 7. We fit cubic-spline interpolating functions to these transfer functions and sampled the interpolating functions to produce a set of 8 linear gray levels in normalized luminance from 1% to 100% of the maximum display luminance. The final set of 8 voltage-controlled gray levels are associated with the electro-distortion curves for the 7 lowest reduced voltages in Figure 6 and the LC cell transmission curves shown in Figure 8. The curves of Figure 8 reflect the optical transmission through all of the LCD optical layers except the thin-film color filters and thus represent LC cell transmission. It is important to recognize the change in shape of the LC cell spectral transmission curves across gray levels, especially in the region below about 500 nm where there are both significant emissions from the illumination source and visual sensitivity.

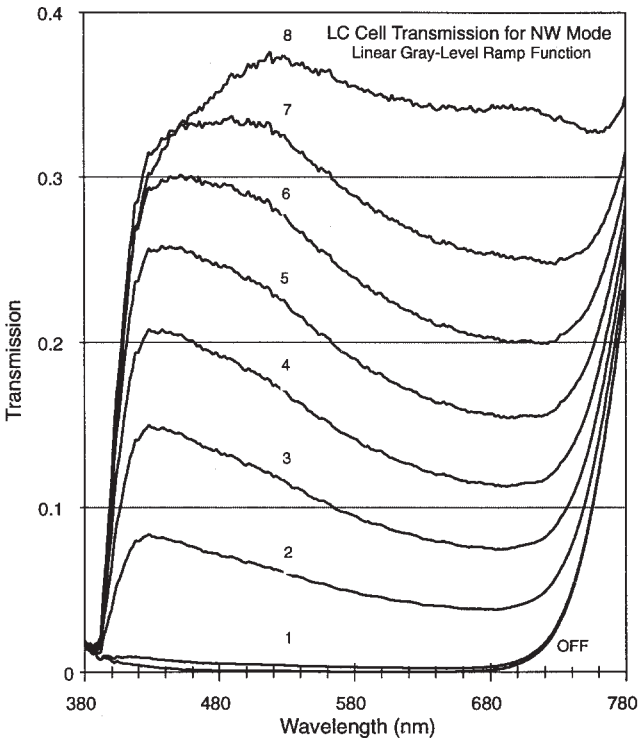

Figure 8. LC cell spectral transmission for the model NW LCD as a function of 8 linear gray levels and the off-state

Color Performance Capabilities and Limits for Current LCD Technology

We have utilized the optical modeling results presented above to calculate the pixel element chromaticity coordinates of the R, G, B primaries of the model LCD as a function of gray levels. These results are presented in Figure 9, which reveals that the chromaticity of R and G pixels are relatively stable across gray levels while the B primary exhibits increasing saturation as display luminance is decreased from 100% to 1% of peak display luminance. These variations in chromaticity may be attri-buted to the changing shape of the LC cell spectral transmission function.

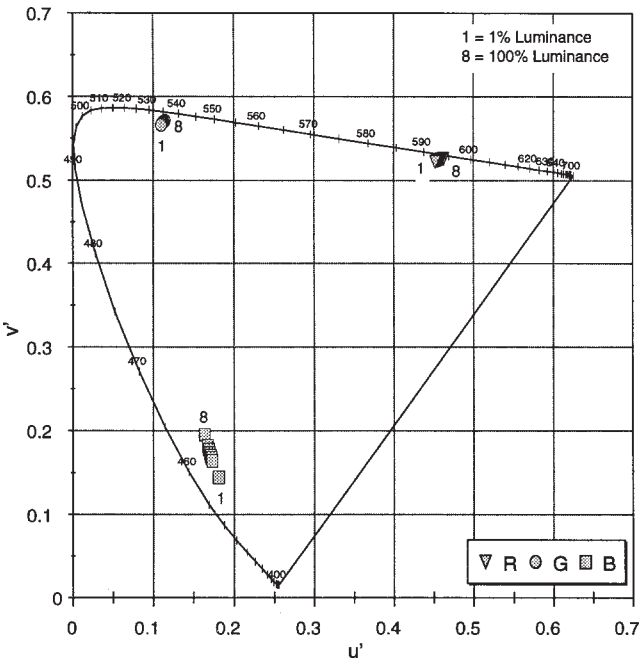

Figure 9. Pixel chromaticity coordinates of the model LCD as a function of gray level

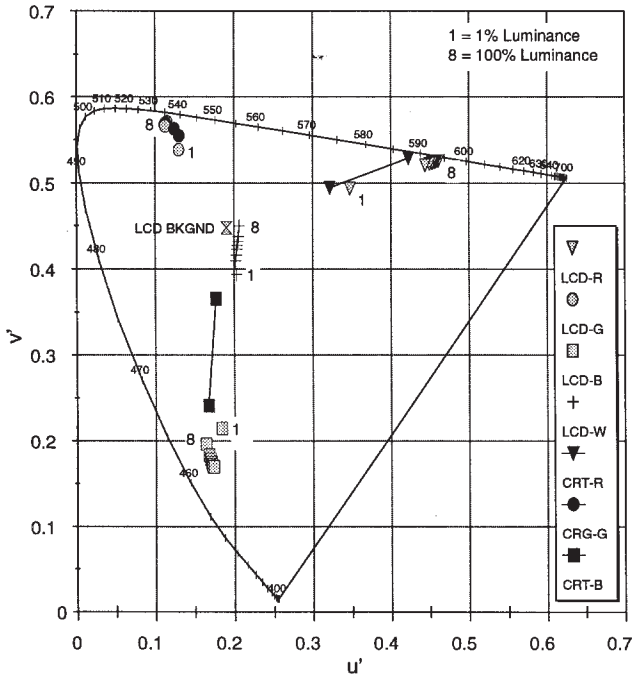

Figure 10. Space-average chromaticity coordinates, white point, and background of the model LCD and a reference CRT as a function of gray level

The final illustration, Figure 10, plots the space-average chromaticity coordinates of the model LCD for the R, G, and B primaries, the display white point, and the display background or off-state as a function of gray levels. For a reference, we have also plotted on this figure the primary chromaticity coordinates of a Barco Calibrator CRT for values of 1% and 100% of its peak luminance.

While the pixel element chromaticity coordinates reflect only the SPDs from individual pixels, the space-average coordinates include the additional contributions of the "leakage" or non-zero off-states of unaddressed pixels. The proportional contributions of these "leakage" effects increase as the gray levels decrease for both the model LCD and the CRT. The space-average chromaticity coordinates are representative of the effective color visual stimulus and thus are more closely correlated with the actual appearance of display colors.

Examination of Figure 10 reveals two important findings. First, the color gamut of the model LCD significantly exceeds that of the high-performance color CRT monitor. Second, the color tracking of the model LCD across gray levels ranging from 1% to 100% of peak display luminance is equivalent to or better than that of the color CRT. Both of these characteristics are vital for color-critical display applications capable of supporting veridical color rendering and the transportability of color across imaging media.

Conclusions

In this paper, we have explored the colorimetric and photometric modeling of LCDs. We have shown that the effective color performance of LCDs can be modeled accurately and that such models can be used to optimize color LCDs for different imaging applications. Most important, we have provided a comprehensive analysis which shows that properly optimized LCDs using existing materials and available LC technology can equal or exceed the color rendering performance of the best of today's color CRT monitors.

Color LCD technology is still relatively new and evolving at a rapid pace. Recent technology demonstrations have unveiled prototype color LCDs with addressable resolution of up to 1536 × 1024 full-color pixels, advanced color synthesis techniques, and remarkable color and image fidelity.[18] Moreover, continuing advances in all key LCD technologies; LC materials, illumination sources, color filters, optical compensation techniques, driver chips and LC controllers, promise to raise the level of performance for each successive generation of color LCDs. Those of us concerned with color imaging can look forward to brighter, higher contrast displays which exceed the color performance of today's color workstation standards.

References

1. Collings, P. J. (1990). *Liquid Crystals: Nature's Delicate Phase of Matter*. Princeton, New Jersey: Princeton University Press.
2. Penz, P. A. (1985). Nonemissive displays. In L. E. Tannas (Ed.), *Flat-Panel Displays and CRTs*. New York: Van Nostrand Reinhold Company, 415-457.
3. Scheffer, T., and Nehring, J. (1990). Twisted nematic and supertwisted nematic mode LCDs. In B. Bahadur (Ed), *Liquid Crystals: Applications and Uses, Volume I*. New Jersey: World Scientific Publishing Company, 231-274.
4. Scheffer, T., and Nehring, J. (1992). Twisted-nematic (TN) and super-twisted nematic LCDs. *Society for Information Display Seminar Lecture Notes*, Volume **I**, M1/1-1/52.
5. Kliger, D. S., Lewis, J. W., and Randall, C. E. (1990). *Polarized Light in Optics and Spectroscopy*. Boston: Academic Press, Inc.
6. Gooch, C. H., and Tarry, H. A. (1975). The optical properties of twisted nematic liquid crystal structures with twist angles <= 90°. *Journal of Applied Physics*, **8**, 1575-1584.
7. Silverstein, L. D. (1991). *Description of an On-Axis Colorimetric/Photometric Model for Twisted-Nematic Color Liquid Crystal Displays*. Unpublished technical report for the NASA/ARPA Visual Display Engineering and Optimization System (ViDEOS) project.
8. Wyszecki, G., and Stiles, W. S. (1982*). Color Science: Concepts and Methods, Quantitative Data and Formulae,* 2nd Edition. New York: John Wiley & Sons, Inc.
9. Yariv, A., and Yeh, P. (1984). *Optical Waves in Crystals*. New York: John Wiley & Sons, Inc.
10. Yeh , P. (1982). Extended Jones matrix method. *Journal of the Optical Society of America*, **72**, 507-513.
11. Ong, H. L. (1991). LCD modeling by 2 x 2 and 4 x 4 propagation matrix methods and by generalized geometrical optics approximation. *Proceedings of the 11th International Display Research Conference*, 1-5.
12. Lien, A. (1990). Extended Jones matrix representation for the twisted-nematic liquid-crystal display at oblique incidence. *Applied Phyics Letters*, **57**, 2767-2769.
13. Berreman, D. W. (1973). Optics in smoothly varying anisotropic planar structures: Application to liquid-crystal twist cells. *Journal of the Optical society of America*, **63**, 1374-1380.
14. Berreman, D. W. (1972). Optics in stratified and anisotropic media. *Journal of the Optical Society of America*, **62**, 502-510.
15. Wohler, H., Haas, G., Fritsch, M., and Mlynski, D. A. (1988). Faster 4 x 4 matrix method for uniaxial inhomogeneous media. *Journal of the Optical Society of America*, **5**, 1554-1556.
16. Berreman, D. W. (1983). Numerical modeling of twisted nematic devices. *Philosophical Transactions of the Royal Society of London*, **309**, 203216.
17. Fiske, T. G., & Silverstein, L. D. (1993). Characterization of viewing-angle dependent colorimetric and photometric performance of color LCDs. *Society for Information Display Technical Digest*, 565-568.
18. Martin, R. A., Chuang, H., Steemers, H., Allen, R., Fulks, R., Stuber, D., Lee, D., Young, M., Ho, J., Nguyen, M., Meuli, W., Fiske, T., Bruce, R., Thompson, M., Tilton, M., and Silverstein, L. D. (1993). A 6.3 million pixel AM-LCD. *Society for Information Display Technical Digest*, 704-707.
19. Silverstein, L. D., Krantz, J. H., Gomer, F. E., Yeh, Y., & Monty, R. W. (1990). The effects of spatial sampling and luminance quantization on the image quality of color matrix displays. *Journal of the Optical Society of America A*, **7**, 1955-1968.